Acta Scientiarum
http://www.periodicos.uem.br/ojs/
ISSN on-line: 1807-8621
Doi: 10.4025/actasciagron.v47i1.72576





# Use of visibility graphs for analysis of computed tomography soil images

**Nicéias Silva Vilela[1*], José Domingos Albuquerque Aguiar[2], Tatijana Stosic[1], Rômulo Simões Cezar Menezes[3], Antonio Celso Dantas Antonino[3] and Borko Stosic[1]**

[1]Programa de Pós-graduação em Biometria e Estatística Aplicada, Departamento de Estatística e Informática, Universidade Federal Rural de Pernambuco, Av. Prof. Moraes Rego, 1235, Cidade Universitária, 50670-901, Recife, Pernambuco, Brazil. [2]Instituto Federal de Educação, Ciência e Tecnologia de Pernambuco, Recife, Pernambuco, Brazil. [3]Departamento de Energia Nuclear, Universidade Federal de Pernambuco, Recife, Pernambuco, Brazil. *Author for correspondence. E-mail: niceias.svilela@gmail.com

**ABSTRACT.** A complex network analysis of three-dimensional soil images obtained by X-ray computed tomography (CT) was employed to analyze the morphological properties of soil under different vegetation covers. This study quantitatively assessed changes in the three-dimensional soil structure due to disturbances caused by sugarcane management techniques. We used CT images of soil covered by the Atlantic Forest and sugarcane with 624,100 voxel columns each to examine topological indices of the networks generated from the vertical lines of the CT images using the visibility graph (VG) method. The VG method successfully described the changes in the structure of the soil samples by comparing the CT images and may be used to quantify soil degradation. The topological indices clustering coefficient, average shortest path, and average degree of the VG network described the communication between soil structural units, pore continuity, and the distribution of paths between pores. We found strong correlations between the phenomenological aspects and the topological descriptors of the generated network, especially for the average degree. This index best highlighted the difference between the samples, revealing greater heterogeneity in the Atlantic Forest sample compared to the sugarcane sample. These correlations indicate that the complexity of the networks of 3D soil images is related to physical properties, enabling quantification of the degradation of soil morphological properties.

**Keywords:** visibility graph; computed tomography; soil.

Received on June 17, 2024.
Accepted on December 1, 2024.

## Introduction

Soil has long been a research priority, as it is vital for sustainable food production and societal well-being. Therefore, soil degradation resulting from economically driven land-use change is a significant concern for the future in many parts of the world. More specifically, land-use change can have negative impacts on essential soil functions, such as nutrient storage, dispersal and recycling, carbon storage and greenhouse gas emissions, disease and pest regulation, erosion resistance, water retention, drainage, and filtration (Bordonal et al., 2018; Bünemann et al., 2018; Creamer et al., 2022; Williams et al., 2020). In turn, economic concerns and population increases are generating a growing need for the use of natural resources in developing countries. In search of pastures, timber, firewood, and areas for cultivation, tropical forests are being converted into agricultural areas at alarming rates. Therefore, a comprehensive assessment of soil properties is essential for the early detection and mitigation of the adverse effects of changes occurring due to these actions.

The impacts of land use changes have been investigated, mainly focusing on physical, chemical, and biological properties (Aon et al., 2001; Das et al., 2018; Ozores-Hampton et al., 2011; Usharani et al., 2019), while fewer studies have been devoted to changes in soil structure (Aguiar et al., 2023; Soto-Gomez et al., 2020). The latter has control over soil functions, and quantification of soil morphology is key to a better understanding of the complex phenomena that rule these functions. In this way, a description and quantification of the soil functions depend on a deep understanding of characteristics such as the three-dimensional distribution of components, their connectivity, hierarchical organization, and complexity.

Recent advances in imaging techniques for assessing soil functions, such as X-ray computed tomography (CT), have proven quite efficient and non-destructive (Soto-Gomez et al., 2020). This technology makes it

possible to examine morphological characteristics through direct observation of the soil structure (Ojeda-Magaña et al., 2014). CT has become a widespread tool for 3D soil visualization and quantification, shedding new light on soil functions (Helliwell et al., 2013). CT has proven to be a powerful tool that provides data that cannot be obtained by other means (Helliwell et al., 2013). These data enhance our understanding of soil structural changes caused by anthropogenic actions (Taina et al., 2008). More precisely, several soil properties that have not previously been amenable to analysis can now be assessed through CT scans, thus providing fundamental new insights into soil functions (Helliwell et al., 2013). These properties include isotropy, homogeneity, complexity, and hierarchical fractal (or multifractal) organization of soil constituents, contributing to a deeper understanding of soil's physical, chemical, and biological processes (Schlüter et al., 2018).

X-ray CT image analysis has already been employed to characterize the spatial distribution of pores, revealing the high complexity of the porous structure (Feng et al., 2020; Iassonov et al., 2009; Ojeda-Magaña et al., 2014; Soto-Gomez et al., 2020). The complexity of the soil structure has also been studied using methods originating from statistical physics, such as fractals and multifractals (Borges et al., 2019; San José Martínez et al., 2017; Soto-Gomez et al., 2020), information theory (Martín et al., 2017), and complex network theory (Samec et al., 2013; Zhang et al., 2019).

From a structural perspective, soil can be defined as an arrangement of solid and void components (Carter, 2004). The arrangement of these components, observed through the attenuation of X-rays, represents a challenge in segmentation. As a consensus has not yet been reached on the appropriate threshold for separating pores from solids in CT images (Tarquis et al., 2009), it was also proposed that instead of using a threshold, grayscale soil images should be used for multifractal characterization of the soil structure (Roy & Perfect, 2014; Torre et al., 2018; Zhou et al., 2011).

The destruction and degradation of natural ecosystems are the main causes of the decline in global biodiversity (Haddad et al., 2015). Brazil is among the most relevant countries in the world in terms of preserved ecosystems and biogenetic richness, housing around 20% of the world's biodiversity. However, multiple factors are responsible for changes in this scenario, and changes in land use are among the most important factors in biodiversity loss (Barlow et al., 2016). From 2000 to 2018, there was a decrease of 489,877 $km^2$ in natural areas in Brazil's six biomes, representing an 8.3% reduction in natural areas throughout the country. Among them, the Atlantic Forest is the biome that shows the highest percentage of degradation over time since it encompasses the most industrialized and productive areas, in addition to having the highest population density in the national territory, housing around 49.3% of the country's urban areas (Instituto Brasileiro de Geografia e Estatística [IBGE], 2020). Sugarcane is one of the most prominent crops in the Atlantic Forest biome region, especially in the Brazilian Northeast, where cultivation is present in eight of the region's nine states. For the 2022/2023 harvest, an increase of 2.9% in the planted area and 12.5% in production was estimated with respect to the previous sugarcane harvest in the northeast region of Brazil (Companhia Nacional de Abastecimento [CONAB], 2023).

The replacement of native Atlantic Forest vegetation by sugarcane cultivation has negative impacts on the physical soil properties (Bordonal et al., 2018; Cherubin et al., 2015; Franco et al., 2016; Haghighi et al., 2010). These properties are responsible for several soil functions, such as water retention and absorption, gaseous processes, erosion prevention, nutrient cycling, and root growth (Rabot et al., 2018), exerting a direct influence on the ecosystem.

In this work, we investigated how land use change affects the soil structure using complex network theory to quantify the complexity of X-ray CT of soil samples. For the first time, the visibility graph method (VG) (Lacasa et al., 2008), introduced to characterize a series (one-dimensional dataset) by mapping it onto a graph, was applied in the context of soil complexity. In this study, the "data" consisted of a set of 790×790 one-dimensional vertical lines of 790 grayscale values in X-ray CT images of soil samples from a sugarcane field and a nearby site in the Atlantic Forest, in northeastern Brazil. For each image and each of the 790×790=624100 generated networks, we calculated topological indices that quantify the structure of the one-dimensional data (Zou et al., 2019). These indices were used to distinguish between samples from the sugarcane plantation and the Atlantic Forest.

## Material and methods

### Data description

Soil samples were collected from a sugarcane field and a nearby area of native Atlantic Forest, located in the state of Pernambuco in the northeastern region of Brazil. The sugarcane fields replaced the original

Atlantic Forest vegetation at least 60 years before the present study and have been continuously cultivated with sugarcane ever since. The soil at the sampling point was classified as a Latossolo in the Brazilian soil classification system, equivalent to Ferralsol in the World Reference Base for Soil Resources (WRB) or Oxisol in the United States Soil Taxonomy System. Samples were collected from the 0–10 cm soil layer using a soil auger containing an internal PVC cylinder measuring 7.5 cm in height by 7.5 cm in diameter. The procedure consisted of excavating the soil by means of careful penetration, with the cylinder attached to a blade. After inserting the auger into the soil, the cylinders were meticulously extracted to preserve the original structure of the environment contained in the PVC cylinders. In the sugarcane fields, samples were collected between the planting rows. For the present study, only one soil sample from the sugarcane field and one sample from the Atlantic Forest area were used to generate the images using X-ray microtomography. After collection, the samples were subjected to 40ºC to remove excess water before performing scanning tomography. CT was performed using third-generation Nikon XT H 225 ST X-ray microtomography equipment (Tring, Hertfordshire, England), operating at a voltage of 150 kV, current of 180 µA, exposure time of 500 ms, and resolution of 45 µm for voxels. A copper filter with a thickness of 0.5 mm was used to reduce low-intensity photons. After scanning the total volume of the cylinder in the initial phase of acquisition, a sub-volume of interest was delimited and recreated using CTPro 3D XT 3.0.3 software (Nikon Metrology NV). The central part of the cylinder was extracted to avoid interference from the edges. The axial 2D reconstructions maintained the 45 µm spatial resolution of the original acquisition and were stored at a 16-bit radiometric resolution (grayscale levels). The resulting volume was 790 stacks with 790×790 pixels, with a resulting volume of $790^3$ = 493,039,000 voxels.

The voxel values of CT images refer to the local density of the sample, and the sequence of values in the vertical direction (gravity), in this situation, considered naturally preferable from a phenomenological point of view, was treated as a one-dimensional dataset, or as a time series of values seen by a virtual observer traveling at constant speed down the vertical direction.

## Transformation of one-dimensional data into complex networks

To analyze the images, a method for mapping one-dimensional data (such as a time series) onto complex networks was adopted. Complex networks are networks that have significant and non-trivial topological characteristics, exhibiting connection patterns between their elements that are neither completely regular nor completely random and composed of nodes and links. A number of methods have been developed to transform a time series into a complex network, with each node representing numerical values in the time series and the weight of a link between any two nodes corresponding to an appropriate quantitative relation (Yu, 2013); that is, the study of the complex networks has been focused on graph theory (Bollobás, 2013).

An undirected or directed graph (Figure 1) is represented by $G = (N, L)$, where the elements of $N \equiv \{n_1, n_2, ..., n_m\}$ are the nodes (or vertices) of the graph $G$, while the elements of $L \equiv \{l_1, l_2, ..., l_k\}$ are the links (or connections or edges). In an undirected graph, each edge between nodes $i$ and $j$, is denoted by $(i, j)$ or $l_{ij}$, and these nodes are referred to as adjacent or neighboring. In a directed graph, the order of the two nodes is important: $l_{ij}$ represents an edge from $i$, to $j$ and $l_{ij} \neq l_{ji}$ (Boccaletti et al., 2006). A common way to visualize a graph is by representing each node by means of a point, and the connections are indicated by connecting two points with a line.

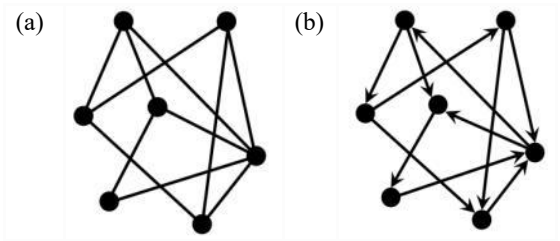


**Figure 1.** Representation of an undirected (a) and directed (b) graph. Source: Boccaletti et al. (2006).

According to Zou et al. (2019), there are several classes of complex networks available for time series analysis based on network construction criteria, such as:

(i) Mutual statistical similarity or metric proximity between different segments of a time series;
(ii) Convexity of successive observations;
(iii) Probability of transition between discrete states.

In the first class, the similarity (or proximity) relationship between different parts of the trajectory of a dynamic system is used to construct the network. A relevant example is recurrence networks. The second class covers visibility graphs and associated concepts, while the third class encompasses transition networks, which are based on ideas from symbolic dynamics and stochastic processes (Zou et al., 2019).

## Visibility graph

Lacasa et al. (2008) introduced an innovative methodology for characterization of time series in complex networks called the Visibility Graph (VG). The VG transforms time series into a graph, where each node corresponds to the data of the original series, and the connection (link) between two nodes is established based on the following geometric visibility criterion.

Let $y_a < y_b$ be two values of the time series observed at time $t_a$ and $t_b$, with $t_a < t_b$. They are visible to each other (and consequently are connected nodes of the graph), if all other data $y_c$ observed at time $t_c$ between such that $t_a < t_c < t_b$ satisfy the following rule:

$$y_c < y_b + (y_a - y_b)\frac{t_a - t_c}{t_b - t_a} \quad (1)$$

In the associated graph, each node "sees" at least its neighbors immediately to the right and left. The graph is undirected (there is no defined direction of the links) and is invariant to affine transformations of the data series, i.e., the visibility criterion is unchanged under the rescaling of the horizontal and vertical axes and under horizontal and vertical translations (Lacasa et al., 2008). An example of a time series containing 20 data values, and the graph derived from the visibility algorithm associated with it are shown in Figure 2. In the graph, each node corresponds sequentially to the data in the original series. The connections between the nodes are defined by the visibility radii between the data.

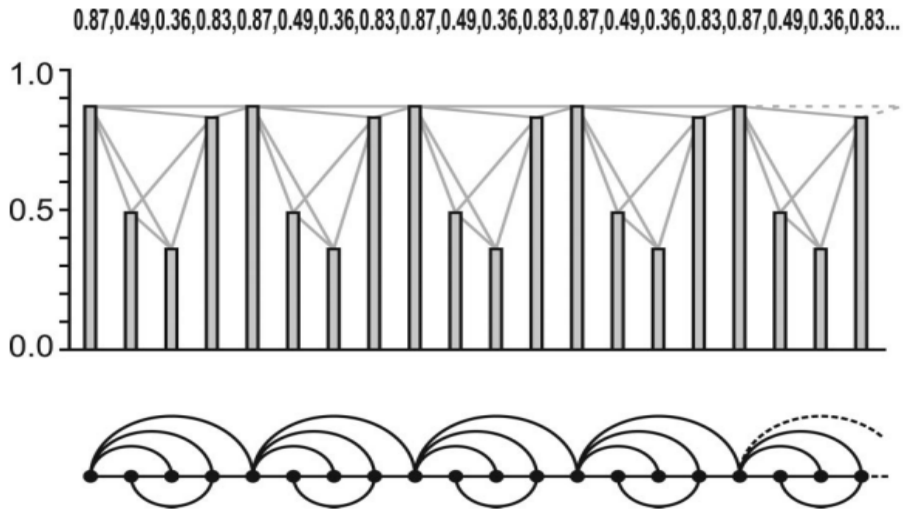


**Figure 2.** An illustrative example of a time series, which is represented by vertical bars (at the top), and its corresponding visibility graph is generated by the VG algorithm (at the bottom). Source: Lacasa et al. (2008).

## Topological indices of the visibility graph

A network generated from the VG algorithm can be represented by its adjacency matrix $A = [a_{ij}]$ where $a_{ij} = 1$ if the nodes $i$ and $j$ are connected and, $a_{ij} = 0$, otherwise. The matrix $A$ can be used to calculate the topological properties of the network (Lacasa et al., 2008; Luque et al., 2009), such as clustering coefficient $C$, average shortest path $\langle d_{ij} \rangle$, and average degree $\langle k \rangle$, which are the indices calculated in this study. The analysis of the topological indices of complex networks permits quantitative analysis of the morphological structure that governs the one-dimensional data (vertical columns of voxels) of the 3D images of the soil samples under study.

The definition of the clustering coefficient was proposed by Watts and Strogatz (1998) to quantify the probability of nodes creating united groups with a relatively high density of connections. The clustering coefficient $C$ is defined as follows: Suppose a node $i$ has $k_i$ neighbors such that at most $k_i \frac{(k_i-1)}{2}$ edges can exist between them (this occurs when all of its neighbors $i$ are connected to all other neighbors). Therefore, the

ratio of the number of connections ($E_i$) that actually exists between these neighboring nodes $k_i$ and the total number $k_i \frac{(k_i-1)}{2}$ gives the local clustering coefficient, defined as:

$$C_i = \frac{2E_i}{k_i-(k_i-1)} \quad (2)$$

The average value of the clustering coefficient $C$ of all nodes is called the clustering coefficient of the network, defined as:

$$C = \frac{1}{n}\sum_{i=1}^{n} C_i \quad (3)$$

where $n$ is the number of nodes in the network. By definition $0 \leqslant C_i \leqslant 1$ and $0 \leqslant C \leqslant 1$.

The average shortest path is a fundamental measure of separation between two nodes in the graph (Boccaletti et al., 2006). This measure reveals the level of integration of a graph and the ease with which information or other entities can be transported through the network. This topological index is given by the average of the shortest paths between all possible pairs of nodes:

$$\langle d_{ij} \rangle = \frac{1}{N(N-1)}\sum_{ij} d_{ij} \quad (4)$$

Where $d_{ij}$ is the shortest distance between nodes $i$ and $j$, that is, the number of edges traveled on the shortest path to get from $i$ to $j$ (Stam & Reijneveld, 2007). The shorter this length, the greater the integration of the network and the more efficient the transport of information within it.

In a graph, the different nodes may present variations in the number of connections, and this quantity is the denominated node degree. The degree is a principal characteristic of a network since it allows the derivation of several relevant measures (Yu, 2013). The average degree is the average value of degrees of all nodes in the complex network.

## Results and discussion

The topological indices of the VG network for soil samples with sugarcane and Atlantic Forest cover are presented in Table 1 (descriptive statistics), Figure 3 (spatial distribution in the horizontal plane), and Figure 4 (histograms).

Table 1 shows that the average degree revealed the greatest difference between the two samples. All values were higher for the Atlantic Forest, indicating a greater number of connections between the network nodes. For soil covered by sugarcane, these connections decreased, reflecting the degradation of morphological properties caused by changes in land use. This can be confirmed in Figure 4, as: i) the histograms of the average length of the shortest path values overlap; this index is not indicated to quantify soil degradation; ii) the clustering coefficient and average degree indices show well-separated histograms, which are more separated for the average degree. The spatial distribution (in the horizontal plane) of the topological indices showed greater heterogeneity for the Atlantic Forest sample than for sugarcane (Figure 3), being more heterogeneous for the average degree index. These results indicate that in VG analysis, the average degree index was more used to quantify the level of soil degradation caused by the change in vegetation cover. This work is a pilot study showing that the VG method is promising for analyzing soil structure through the influence of its use. As only two samples were used (one for each with vegetation cover), more samples need to be compared to confirm the validity of this approach through statistical tests.

**Table 1.** Descriptive statistics of the topological measures of the VG network obtained from the soil sample covered by sugarcane (SC) and the Atlantic Forest (AF).

| Descriptive statistics | Topological indexes | | | | | |
|---|---|---|---|---|---|---|
| | Clustering coefficient $C$ | | Average shortest path $\langle d_{ij} \rangle$ | | Average degree $\langle k \rangle$ | |
| | SC | AF | SC | AF | SC | AF |
| Mean | 0.713 | 0.699 | 4.623 | 4.648 | 10.340 | 12.437 |
| Standard deviation | 0.007 | 0.008 | 0.285 | 0.303 | 0.479 | 0.742 |
| Minimum | 0.672 | 0.659 | 2.899 | 2.920 | 8.562 | 9.316 |
| 1st Quartile | 0.708 | 0.694 | 4.474 | 4.478 | 10.020 | 11.916 |
| Median | 0.713 | 0.699 | 4.626 | 4.643 | 10.299 | 12.380 |
| 3rd Quartile | 0.718 | 0.705 | 4.790 | 4.825 | 10.605 | 12.889 |
| Maximum | 0.745 | 0.738 | 6.270 | 7.131 | 16.448 | 19.562 |

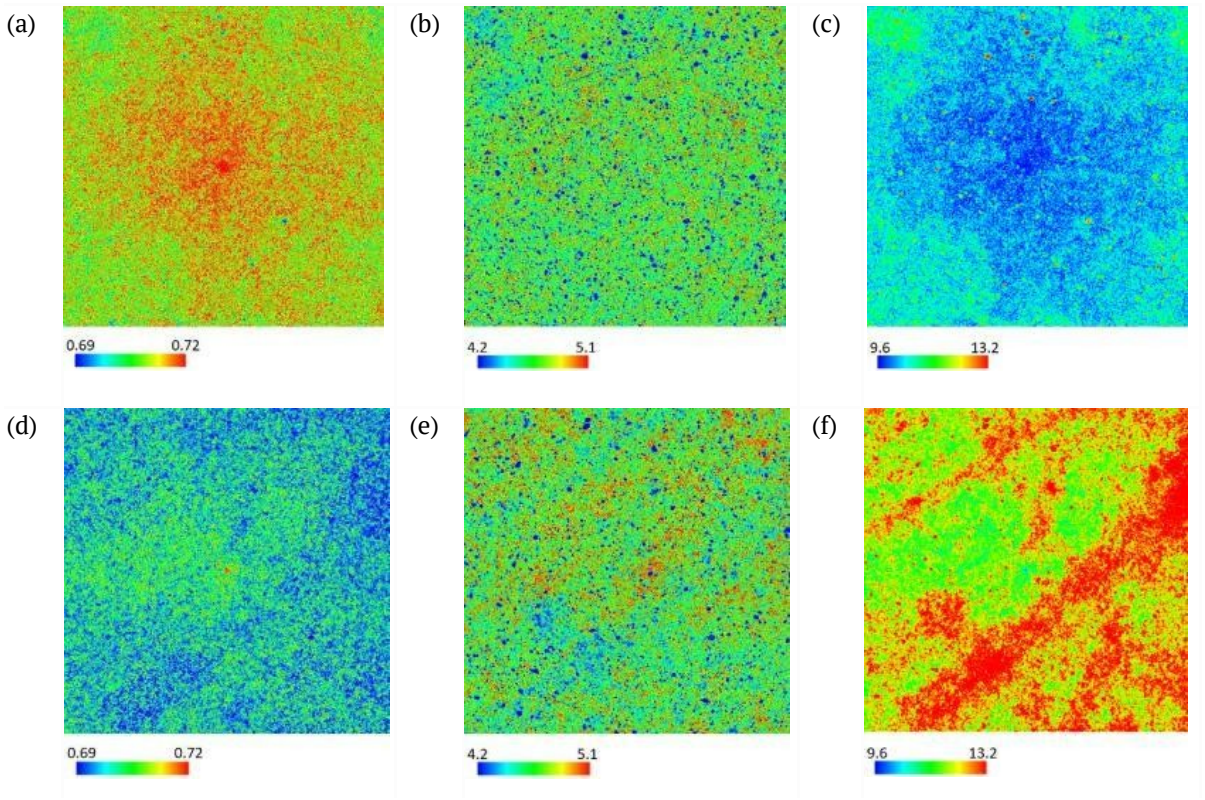


**Figure 3.** Color-coded VG index values of the soil sample with sugarcane cover, (a) clustering coefficient (b) average shortest path, and (c) average degree; and with Atlantic Forest cover, (d) clustering coefficient (e) average shortest path, and (f) average degree. The color-coding scheme was chosen to emphasize the contrast between the topological measurements of the samples, with limits corresponding to ±1.5 standard deviations of the composite sample, and the composite mean.

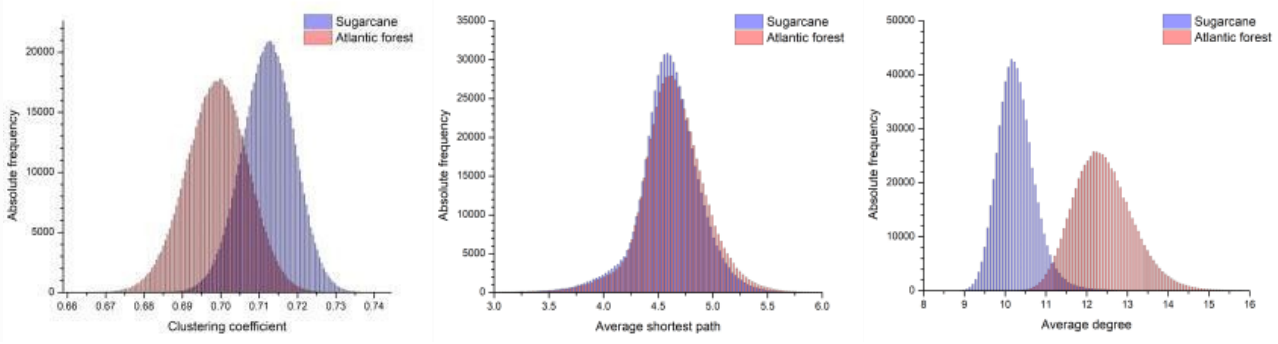


**Figure 4.** Histograms of the indices calculated from the VG metrics for the two samples.

## Conclusion

This work presented the use of the VG method from complex network theory to analyze the structure of CT images of soil covered by sugarcane and the Atlantic Forest. Based on the analysis of VG topological indices, it can be concluded that: i) Calculated for each vertical line of voxels, the clustering coefficient and average shortest path indicated that the change in vegetation cover—conversion of native forest to sugarcane—altered the morphological properties of the soil in the direction of greater homogeneity, greater connectivity, and efficiency of information transport of the networks. ii) The average degree showed the greatest difference between the two samples. In this context, it stood out as the index most used to quantify the degradation of soil morphological properties caused by changes in vegetation cover. The results of this study may be useful for developing and validating theoretical and computational models for studying soil structures. The VG method, which had not been applied to the study of three-dimensional soil images until now, proved efficient in capturing the structural properties of networks generated from one-dimensional data, such as a time series, which here was the vertical lines of voxels of the CT images. In future work, other topological measures of visibility graphs can be explored and used to study soil structure behavior.

Furthermore, variations of the VG method can be applied, such as the horizontal visibility graph (Luque et al., 2009), limited penetrable horizontal visibility graph (Wang et al., 2018), weighted visibility graph (Supriya et al., 2016), and multiscale visibility graph (Li & Zhao, 2018).

## Data availability

Not applicable.

## Acknowledgements

The authors acknowledge support from the Brazilian agency FACEPE (grants: APQ-0498-3.07/17 INCT 2014, APQ-0500-5.01/22; CNPq 406202/2022-2). T. Stosic and B. Stosic acknowledge support from Brazilian agency CNPq (grants No 308782/2022-4 and 309499/2022-4). B. Stosic acknowledges support of Brazilian agency CAPES through grant No. 88887.937789/2024-00.

## References

Aguiar, D., Menezes, R. S. C., Antonino, A. C. D., Stosic, T., Tarquis, A. M., & Stosic, B. (2023). Quantifying soil complexity using Fisher Shannon method on 3D X-ray computed tomography scans. *Entropy*, *25*(10), 1-16. https://doi.org/10.3390/e25101465

Aon, M. A., Sarena, D. E., Burgos, J. L., & Cortassa, S. (2001). (Micro) biological, chemical and physical properties of soils subjected to conventional or no-till management: An assessment of their quality status. *Soil and Tillage Research*, *60*(3-4), 173-186. https://doi.org/10.1016/S0167-1987(01)00190-8

Barlow, J., Lennox, G. D., Ferreira, J., Berenguer, E., Lees, A. C., Nally, R. M., Thomson, J. R., Ferraz, S. F. B., Louzada, J., Oliveira, V. H. F., Parry, L., Solar, R. R. C., Vieira, I. C. G., Aragão, L. E. O. C., Begotti, R. A., Braga, R. F., Cardoso, T. M., Oliveira Junior, R. C., Souza Junior, C. M., … Gardner, T. A. (2016). Anthropogenic disturbance in tropical forests can double biodiversity loss from deforestation. *Nature*, *535*, 144-147. https://doi.org/10.1038/nature18326

Boccaletti, S., Latora, V., Moreno, Y., Chavez, M., & Hwang, D.-U. (2006). Complex networks: Structure and dynamics. *Physics Reports*, *424*(4-5), 175-308. https://doi.org/10.1016/j.physrep.2005.10.009

Bollobás, B. (2013). *Modern graph theory* (v. 184). Springer Science & Business Media.

Bordonal, R. O., Carvalho, J. L. N., Lal, R., Figueiredo, E. B., Oliveira, B. G., & La Scala Jr., N. (2018). Sustainability of sugar cane production in Brazil. A review. *Agronomy for Sustainable Development*, *38*(13), 1-23. https://doi.org/10.1007/s13593-018-0490-x

Borges, L. P. F., Moraes, R. M., Crestana, S., & Cavalcante, A. L. B. (2019). Geometric features and fractal nature of soil analyzed by X-ray microtomography image processing. *International Journal of Geomechanics*, *19*(8). https://doi.org/10.1061/(ASCE)GM.1943-5622.0001464

Bünemann, E. K., Bongiorno, G., Bai, Z., Creamer, R. E., De Deyn, G., Goede, R., Fleskens, L., Geissen, V., Kuyper, T. W., Mader, P., Pulleman, M., Sukkel, W., van Groenigen, J. W., & Brussaard, L. (2018). Soil quality–A critical review. *Soil Biology and Biochemistry*, *120*, 105-125. https://doi.org/10.1016/j.soilbio.2018.01.030

Carter, M. R. (2004). Researching structural complexity in agricultural soils. *Soil and Tillage Research*, *79*(1), 1-6. https://doi.org/10.1016/j.still.2004.04.001

Cherubin, M. R., Franco, A. L. C., Cerri, C. E. P., Silva Oliveira, D. M., Davies, C. A., & Cerri, C. C. (2015). Sugar cane expansion in Brazilian tropical soils-Effects of land use change on soil chemical attributes. *Agriculture, Ecosystems & Environment*, *211*, 173-184. https://doi.org/10.1016/j.agee.2015.06.006

Creamer, R. E., Barel, J. M., Bongiorno, G., & Zwetsloot, M. J. (2022). The life of soils: Integrating the who and how of multifunctionality. *Soil Biology and Biochemistry*, *166*, 1-15. https://doi.org/10.1016/j.soilbio.2022.108561

Companhia Nacional de Abastecimento [CONAB]. (2023). *Acompanhamento da safra brasileira de cana-de-açúcar – Safra 2022/23 - Quarto levantamento*. CONAB.

Das, A., Lyngdoh, D., Ghosh, P. K., Lal, R., Layek, J., & Idapuganti, R. G. (2018). Tillage and cropping sequence effect on physico-chemical and biological properties of soil in Eastern Himalayas, India. *Soil and Tillage Research*, *180*, 182-193. https://doi.org/10.1016/j.still.2018.03.005

Feng, Y., Wang, J., Bai, Z., Reading, L., & Jing, Z. (2020). Three-dimensional quantification of macropore networks of different compacted soils from opencast coal mine area using X-ray computed tomography. *Soil and Tillage Research*, *198*, 104567. https://doi.org/10.1016/j.still.2019.104567

Franco, A. L. C., Bartz, M. L. C., Cherubin, M. R., Baretta, D., Cerri, C. E. P., Feigl, B. J., Wall, D. H., Davies, C. A., Cerri, C. C. (2016). Loss of soil (macro) fauna due to the expansion of Brazilian sugar cane acreage. *Science of the Total Environment*, *563-564*, 160-168. https://doi.org/10.1016/j.scitotenv.2016.04.116

Haddad, N. M., Brudvig, L. A., Clobert, J., Davies, K. F., Gonzalez, A., Holt, R. D., Lovejoy, T. E., Sexton, J. O., Austin, M. P., Collins, C. D., Cook, W. M., Damschen, E. I., Ewers, R. M., Foster, B. L., Jenkins, C. N., King, A. J., Laurance, W. F., Levey, D. J., Margules, C. R., ... Townshend, J. R. (2015). Habitat fragmentation and its lasting impact on Earth's ecosystems. *Science Advances*, *1*(2), 1-9. https://doi.org/10.1126/sciadv.150005

Haghighi, F., Gorji, M., & Shorafa, M. (2010). A study of the effects of land use changes on soil physical properties and organic matter. *Land Degradation & Development*, *21*(5), 496-502. https://doi.org/10.1002/ldr.999

Helliwell, J. R., Sturrock, C. J., Grayling, K. M., Tracy, S. R., Flavel, R. J., Young, I. M., Whalley, W. R., & Mooney, S. J. (2013). Applications of X-ray computed tomography for examining biophysical interactions and structural development in soil systems: A review. *European Journal of Soil Science*, *64*(3), 279-297. https://doi.org/10.1111/ejss.12028

Iassonov, P., Gebrenegus, T., & Tuller, M. (2009). Segmentation of X-ray computed tomography images of porous materials: A crucial step for characterization and quantitative analysis of pore structures. *Water Resources Research*, *45*(9), 1-12. https://doi.org/10.1029/2009WR008087

Instituto Brasileiro de Geografia e Estatística [IBGE]. (2020). *Coordenação de recursos naturais e estudos ambientais, coordenação de contas nacionais. Contas de ecossistemas: o uso da terra nos biomas brasileiros: 2000-2018*. IBGE.

Lacasa, L., Luque, B., Ballesteros, F., Luque, J., & Nuno, J. C. (2008). From time series to complex networks: The visibility graph. *Proceedings of the National Academy of Sciences*, *105*(13), 4972-4975. https://doi.org/10.1073/pnas.0709247105

Li, W., & Zhao, X. (2018). Multiscale horizontal-visibility-graph correlation analysis of stock time series. *Europhysics Letters*, *122*(4), 40007. https://doi.org/10.1209/0295-5075/122/40007

Luque, B., Lacasa, L., Ballesteros, F., & Luque, J. (2009). Horizontal visibility graphs: Exact results for random time series. *Physical Review E*, *80*(4), 046103. https://doi.org/10.1103/PhysRevE.80.046103

Martín, M. Á., Reyes, M., & Javier Taguas, F. (2017). Estimating soil bulk density with information metrics of soil texture. *Geoderma*, *287*, 66-70. https://doi.org/10.1016/j.geoderma.2016.09.008

Ojeda-Magaña, B., Quintanilla-Domínguez, J., Ruelas, R., Tarquis, A. M., Gómez-Barba, L., & Andina, D. (2014). Identification of pore spaces in 3D CT soil images using PFCM partitional clustering. *Geoderma*, *217-218*, 90-101. https://doi.org/10.1016/j.geoderma.2013.11.005

Ozores-Hampton, M., Stansly, P. A., & Salame, T. P. (2011). Soil chemical, physical, and biological properties of a sandy soil subjected to long-term organic amendments. *Journal of Sustainable Agriculture*, *35*(3), 243-259. https://doi.org/10.1080/10440046.2011.554289

Rabot, E., Wiesmeier, M., Schlüter, S., & Vogel, H.-J. (2018). Soil structure as an indicator of soil functions: A review. *Geoderma*, *314*, 122-137. https://doi.org/10.1016/j.geoderma.2017.11.009

Roy, A., & Perfect, E. (2014). Lacunarity analyses of multifractal and natural grayscale patterns. *Fractals*, *22*(03), 1440003. https://doi.org/10.1142/S0218348X14400039

Samec, M., Santiago, A., Cárdenas, J. P., Benito, R. M., Tarquis, A. M., Mooney, S. J., & Korošak, D. (2013). Quantifying soil complexity using network models of soil porous structure. *Nonlinear Processes in Geophysics*, *20*(1), 41-45. https://doi.org/10.5194/npg-20-41-2013

San José Martínez, F., Caniego, F. J., & García-Gutiérrez, C. (2017). Lacunarity of soil macropore space arrangement of CT images: Effect of soil management and depth. *Geoderma*, *287*, 80-89. https://doi.org/10.1016/j.geoderma.2016.09.007

Schlüter, S., Großmann, C., Diel, J., Wu, G.-M., Tischer, S., Deubel, A., & Rücknagel, J. (2018). Long-term effects of conventional and reduced tillage on soil structure, soil ecological and soil hydraulic properties. *Geoderma*, *332*, 10-19. https://doi.org/10.1016/j.geoderma.2018.07.001

Soto-Gomez, D., Perez-Rodriguez, P., Juiz, L. V., Paradelo, M., & Lopez-Periago, J. E. (2020). 3D multifractal characterization of computed tomography images of soils under different tillage management: Linking multifractal parameters to physical properties. *Geoderma*, *363*, 114129. https://doi.org/10.1016/j.geoderma.2019.114129

Stam, C. J., & Reijneveld, J. C. (2007). Graph theoretical analysis of complex networks in the brain. *Nonlinear Biomedical Physics*, *1*(3), 1-19. https://doi.org/10.1186/1753-4631-1-3

Supriya, S., Siuly, S., Wang, H., Cao, J., & Zhang, Y. (2016). Weighted visibility graph with complex network features in the detection of epilepsy. *IEEE Access*, *4*, 6554-6566. https://doi.org/10.1109/ACESSO.2016.2612242

Taina, I. A., Heck, R. J., & Elliot, T. R. (2008). Application of X-ray computed tomography to soil science: A literature review. *Canadian Journal of Soil Science*, *88*(1), 1-20. https://doi.org/10.4141/CJSS06027

Tarquis, A. M., Heck, R. J., Andina, D., Alvarez, A., & Antón, J. M. (2009). Pore network complexity and thresholding of 3D soil images. *Ecological Complexity*, *6*(3), 230-239. https://doi.org/10.1016/j.ecocom.2009.05.010

Torre, I. G., Losada, J. C., & Tarquis, A. M. (2018). Multiscaling properties of soil images. *Biosystems Engineering*, *168*, 133-141. https://doi.org/10.1016/j.biosystemseng.2016.11.006

Usharani, K. V., Roopashree, K. M., & Naik, D. (2019). Role of soil physical, chemical and biological properties for soil health improvement and sustainable agriculture. *Journal of Pharmacognosy and Phytochemistry*, *8*(5), 1256-1267. https://doi.org/10.22271/phyto

Watts, D. J., & Strogatz, S. H. (1998). Collective dynamics of 'small-world' networks. *Nature*, *393*(6684), 440-442. https://doi.org/10.1038/30918

Wang, M., Vilela, A. L. M., Du, R., Zhao, L., Dong, G., Tian, L., & Stanley, H. E. (2018). Topological properties of the limited penetrable horizontal visibility graph family. *Physical Review E*, *97*(5), 052117. https://doi.org/10.1103/PhysRevE.97.052117

Williams, H., Colombi, T., & Keller, T. (2020). The influence of soil management on soil health: An on-farm study in southern Sweden. *Geoderma*, *360*, 1-9. https://doi.org/10.1016/j.geoderma.2019.114010

Yu, L. (2013). Visibility graph network analysis of gold price time series. *Physica A: Statistical Mechanics and its Applications*, *392*(16), 3374-3384. https://doi.org/10.1016/j.physa.2013.03.063

Zhang, Z., Wang, J., & Li, B. (2019). Determining the influence factors of soil organic carbon stock in opencast coal-mine dumps based on complex network theory. *Catena*, *173*, 433-444. https://doi.org/10.1016/j.catena.2018.10.030

Zhou, H., Perfect, E., Lu, Y. Z., Li, B. G., & Peng, X. H. (2011). Multifractal analyses of grayscale and binary soil thin section images. *Fractals*, *19*(03), 299-309. https://doi.org/10.1142/S0218348X11005403

Zou, Y., Donner, R. V., Marwan, N., Donges, J. F., & Kurths, J. (2019). Complex network approaches to nonlinear time series analysis. *Physics Reports*, *787*, 1-97. https://doi.org/10.1016/j.physrep.2018.10.005